Response of Hot-Element Wall Shear-Stress Gages in Laminar Oscillating Flows

William J. Cook* and Timothy A. Giddings†
Iowa State University, Ames, Iowa
and
John D. Murphy‡
NASA Ames Research Center, Moffett Field, California

An experimental investigation of the time-dependent response of hot-element wall shear-stress gages in unsteady periodic airflows is reported. The study has focused on wall shear stress for laminar oscillating flows produced on a flat plate by a freestream velocity composed of a mean component and a superposed sinusoidal variation since the wall shear-stress variation for these flows can be predicted numerically with reasonable accuracy. Two types of hot element gages, platinum-film and flush-wire, were tested for values of reduced frequency $\bar{\omega} = \omega x/U_0$ ranging from 0.14 to 2.36. Values of ϕ_τ, the phase angle of the wall shear-stress variation relative to the freestream velocity, as indicated by the hot-element gages, are compared with corresponding numerically determined values of ϕ_τ for the flows, since agreement would indicate that the gages faithfully follow the true wall shear-stress variation. The comparisons show that the gages indicate a wall shear-stress variation that lags the true variation. The time lag, which was found to exist even at low values of $\bar{\omega}$, is attributed primarily to unsteady heat-conduction effects in the gage substrate. Results indicate that a frequency-response correction to gage output is required in order to interpret gage response.

Nomenclature

f	= frequency, Hz
OHR	= hot-element resistance ratio, R/R_a
R	= hot-element resistance
R_a	= element resistance at room temperature
Re	= Reynolds number, $U_0 x/\nu$
t	= time
u	= x component of boundary-layer velocity
U	= freestream velocity
x	= distance from plate leading edge
y	= distance perpendicular to plate surface
β	= pressure-gradient parameter, Eq. (4)
ν	= kinematic viscosity
τ	= wall shear stress
ϕ	= phase angle
ω	= angular frequency, $2\pi f$
$\bar{\omega}$	= reduced frequency, $\omega x/U_0$
δ	= boundary-layer velocity thickness
η	= dimensionless distance $y\sqrt{U_0/\nu x}$

Subscripts

0	= mean value
1	= amplitude
e	= experimental quantity
ex	= obtained by extrapolation
n	= numerically determined quantity
u	= velocity quantity
τ	= wall shear-stress quantity

Presented as Paper 86-1100 at the AIAA/ASME 4th Fluid Mechanics, Plasma Dynamics, and Lasers Conference, Atlanta, GA, May 12-14, 1986; received July 22, 1986; revision received Aug. 28, 1987.

*Professor, Mechanical Engineering Department. Member AIAA.
†Graduate Student, Mechanical Engineering Department.
‡Research Scientist.

Introduction

ONE of the basic quantities of interest in fluid dynamics is surface shear stress. A challenge in experimental fluid mechanics is the measurement of this quantity, particularly for unsteady flows. For steady flows, several instruments and techniques are available.[1] Prominent among these in aerodynamic testing is the floating-element balance.[2] However, many of the instruments used for measuring steady-flow wall shear stress have long response times, e.g., the floating-element balance, and thus are not suitable for measurements in flows with appreciable unsteady effects. One instrument that appears to have the response characteristics for wall shear-stress measurement in time-dependent flows is the hot-element gage. This instrument is illustrated in Fig. 1. The gage surface is mounted flush with the wall on which shear stress is to be measured and the hot element is oriented with its long dimension perpendicular to the flow as shown in the figure. It is operated by a constant temperature anemometer unit identical to that used in hot-wire anemometry.

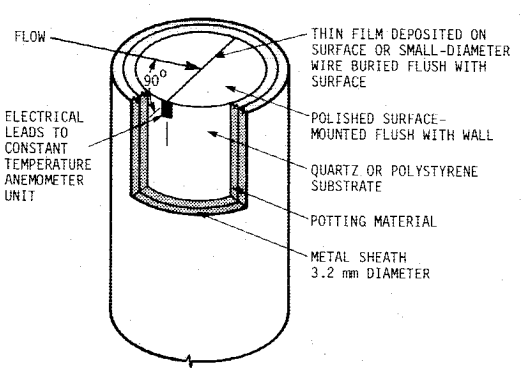

Fig. 1 Hot-element gage description.

The principle of operation stems from the fact that the instantaneous heat transfer from the hot element to the fluid is related to the instantaneous surface shear stress. The anemometer unit senses any change in resistance of the hot element that accompanies a change in its temperature brought about by a change in heat-transfer rate and regulates the electric current flowing through the hot element in order to maintain constant element temperature. Part of the energy dissipated by the hot element is convected away by the flow over the element and part is conducted into the substrate. The instrument is particularly attractive since it is small and relatively easy to use. It has been used by Bellhouse and Schultz[3] to measure the mean and fluctuating wall shear-stress components in an oscillating flow and by other investigators[4-6] in conjunction with a reference freestream hot wire to measure the phase relationship between the freestream velocity variation and the wall shear-stress variation in oscillating turbulent flows. These flows are characterized by a mean freestream velocity with a superposed sinusoidal variation.

In two of these studies,[4,5] there is a discrepancy between the measured phase difference and the expected or predicted difference, indicating possible time-response difficulties with the gages. Literature related to the use of these gages in time-dependent flows is sparse. The study by Bellhouse and Schultz describes use of the gages to measure the mean and varying components of shear stress in an oscillating flow, but does not address the time response of the gages. Possible difficulties with hot-element gage response are discussed by Dewey,[7] Hanratty and Campbell,[8] and Mao and Hanratty.[9] The latter two studies provide a treatment of the influence of fluid-related unsteadiness on the response of probes that rely on either mass or heat transfer as the means of measuring wall shear stress. Experiments in which time-dependent wall shear stress was measured in an oscillating liquid flow with mass-transfer probes are described in Ref. 9.

Menendez and Ramaprian[10] developed analytical relations for the performance of hot-element wall shear-stress gages for application to general unsteady flows, but they note that their results need to be subjected to experimental verification. This seems particularly appropriate since they ignored heat conduction in the substrate. Indeed, time-dependent heat conduction in the substrate appears to be an important factor in gage response. This contention is supported by a study conducted by Cole and Beck,[11] in which an analytical-numerical technique was employed to solve the coupled transient heat-conduction fluid-dynamics problem for a geometry similar to that of the hot-element gage and a step input for heat flux at the element. Their results indicate that conduction in the substrate dominates for air flowing over a gage with a glass substrate. General design considerations for hot-element gages suggest that the element length L in the flow direction be small within certain limits and that the width W, the element dimension perpendicular to the flow, be large compared to L. Furthermore, it appears desirable to use a substrate with a low thermal diffusivity. However, there are no studies, either analytical or experimental, that provide quantitative information on the frequency response of these instruments. The present study was undertaken to examine the time-response characteristics of hot-element gages in oscillating flows. It is primarily experimental in nature. Theoretical analysis of the behavior of hot-element gages is very complex due to two- and possibly three-dimensional time-dependent heat transfer in the substrate that is coupled with the time-dependent effects in the flow over the gage surface.

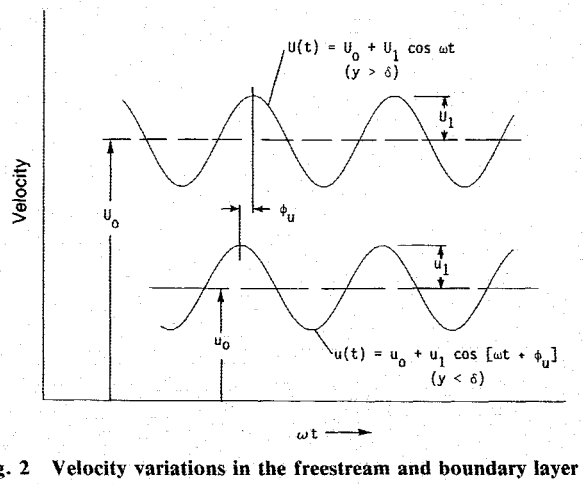

Fig. 2 Velocity variations in the freestream and boundary layer for an oscillating flow.

An experimental investigation of gage response requires either an independent measurement of wall shear stress or a known solution against which experimental results can be compared. The absence of a reliable independent measurement technique suggests obtaining a time-dependent solution for the variation of wall shear stress for an unsteady flow that can be studied experimentally and comparing experimental results with the solution. For turbulent oscillating flows there is, as discussed by Cousteix,[12] considerable uncertainty regarding the time-dependent flow behavior near the wall, and consequently uncertainty in the wall shear stress. This uncertainty, however, does not exist for laminar oscillating flows. Therefore, as a first step in studying response characteristics of these gages, this investigation has focused on the experimental study of the behavior of hot-element gages in laminar oscillating flows and a comparison of experimental results with theoretical predictions for these flows.

Description of Laminar Oscillating Flow

The flow considered is a laminar incompressible flow over a flat plate produced by a freestream velocity composed of a mean value and a sinusoidal oscillating component. The freestream velocity is given by

$$U(t) = U_0 + U_1 \cos\omega t \tag{1}$$

The velocity in the boundary layer is

$$u(y,t) = u_0(y) + u_1(y)\cos[\omega t + \phi_u(y)] \tag{2}$$

where ϕ_u is the phase difference between the boundary-layer and the freestream velocity variations. The velocity variations given by Eqs. (1) and (2) are illustrated in Fig. 2. Positive values of ϕ_u indicate that the boundary-layer velocity variation leads the freestream velocity variation, as shown in the figure. The corresponding wall shear stress is

$$\tau(x,t) = \tau_0(x) + \tau_1(x)\cos[\omega t + \phi_\tau(x)] \tag{3}$$

where ϕ_τ is the phase difference between the wall shear-stress variation and the freestream velocity variation. Agreement between measured and theoretically predicted values for ϕ_τ would indicate correct time response of the hot-element gages. Since the concern here is with the time response of the gages, this study deals only with ϕ_τ. No attempt was made to calibrate the gages in order to determine the mean and oscillating components of the wall shear stress in Eq. (3).

Lighthill[13] was the first to study laminar oscillating flow on a flat plate with a zero-mean pressure gradient. Analytical solutions were obtained for ϕ_τ at low and high values of reduced frequency $\bar{\omega} = \omega x/U_0$. These solutions are shown in Fig. 3 along with numerical solutions for ϕ_τ obtained by Cebeci and Carr[14] and Murphy and Prenter.[15] These results indicate that the wall shear-stress variation leads the freestream velocity variation for all values of $\bar{\omega}$ greater than zero, and that ϕ_τ approaches 45 deg asymptotically as $\bar{\omega}$ increases.

Results from an experimental study of laminar oscillating boundary-layer flows by Hill and Stenning[16] demonstrate that

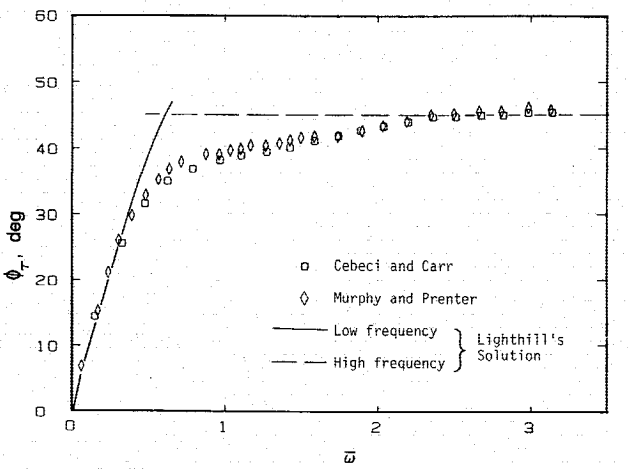

Fig. 3 Predictions for ϕ_τ in oscillating laminar flat plate flow with zero-mean pressure gradient.

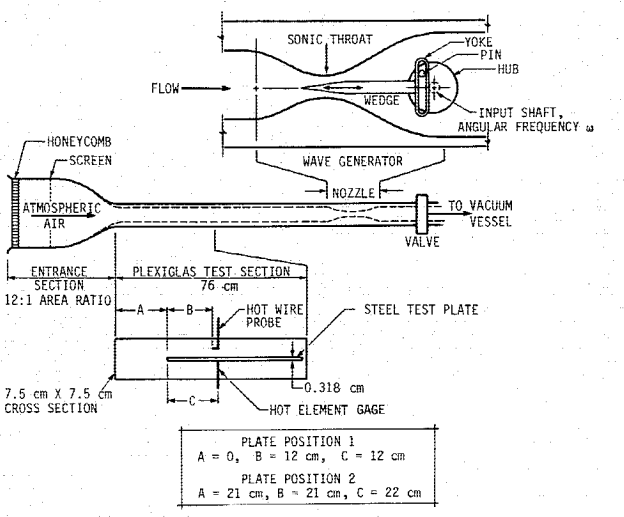

Fig. 5 Diagram of the oscillating-flow facility and test-section arrangement.

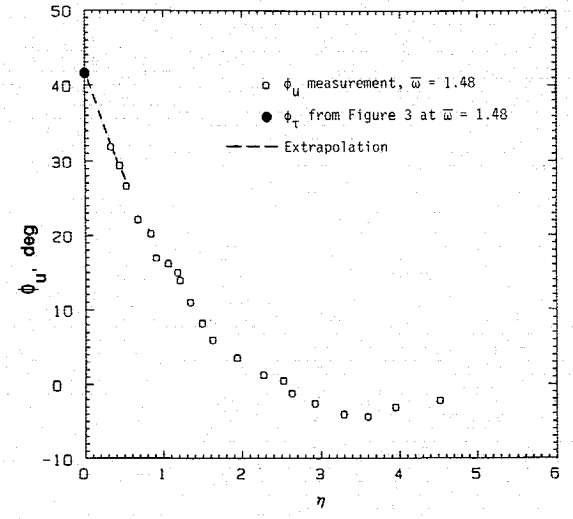

Fig. 4 Experimental results for ϕ_u vs η for a laminar oscillating flow with zero-mean pressure gradient.[16]

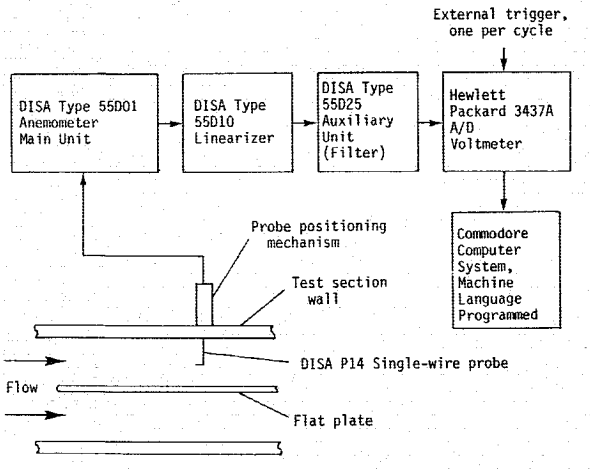

Fig. 6 Data-acquisition system for velocity measurements.

zero-mean pressure-gradient laminar oscillating flows with ϕ_τ as predicted in Fig. 3 can be generated. Figure 4 shows results from one of their zero-mean pressure-gradient cases for ϕ_u vs the similarity variable η. Since the limit of ϕ_u as y approaches zero is ϕ_τ, an experimental value of ϕ_τ can be obtained by extrapolation of the results in Fig. 4 and compared with the corresponding predicted value from Fig. 3. Figure 4 indicates that this extrapolation and the predicted value of ϕ_τ agree very well.

Experimental Facility

The unsteady boundary-layer flow facility in the Iowa State University Mechanical Engineering Department was utilized in this study. A diagram of the facility with the flat plate mounted in the test section is shown in Fig. 5. The entrance section is open to the atmosphere, and the facility is driven by a downstream vacuum source. During operation, the nozzle discharge region pressure is low enough to produce sonic flow at the nozzle throat. When the position of the wedge of the wave generator is fixed, the test-section flow is steady. When the wave generator mechanism is operated, the test-section freestream flow at any x position is characterized by a non-zero-mean velocity and an oscillating component. The mechanism consists of a scotch yoke that imparts sinusoidal axial motion to the wedge when the input shaft is driven at constant speed. As the wedge undergoes motion, the sonic throat area changes, thereby varying the mass rate of flow and producing a wave pattern in the test section. Proper shaping of the wedge will produce a sinusoidal velocity variation. The test-section mean velocity and the amplitude of oscillation are governed by the mean effective sonic area and the variation in sonic area produced by the wedge motion, respectively. The facility has advantages over other types of facilities used to generate unsteady boundary layers in that it produces a sinusoidal velocity variation over a wide range of frequency, and the choked nozzle isolates the test section from downstream flow disturbances. The present experiments involved frequencies ranging from 3 to 20 Hz.

Two freestream oscillating flow conditions were created by use of two configurations of the wave generator. These, in combination with the two test plate positions shown in Fig. 5, formed three test configurations as described in Table 1. The use of three test configurations allowed flows with a wide range of $\bar{\omega}$ to be generated. The ratio of the freestream amplitude of oscillation U_1 to the mean freestream velocity U_0 is given in Table 1 for each test configuration. The flat plate had an elliptical leading edge and was installed horizontally along the centerline of the test section. The plate surface and leading edge were polished to an RMS finish of 15 μ in. in order to ensure laminar flow. Holes were drilled in the plate

Table 1 Description of test configurations

Designation	U_0, m/s	U_1/U_0	Plate position	x, m	Re^a
TC I	16.7	0.13	1	0.12	1.34×10^5
TC II	16.7	0.13	2	0.22	2.35×10^5
TC III	11.7	0.19	2	0.22	1.72×10^5

[a]Based on U_0 and x.

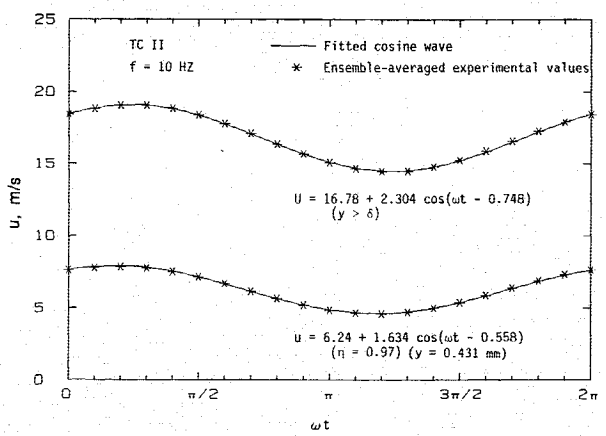

Fig. 7 Cosine wave fits for two velocity variations from boundary-layer survey A4, Table 2. Angles are in rad.

perpendicular to the plate surface to permit the hot-element gages to be installed. The gages were installed through the lower wall of the test section and through these holes. An optical magnifier was used to aid the matching of the gage hot-element surface with the plate surface. A single-element hot-wire probe was used to measure the velocity variation in the freestream and boundary layer. The hot-element and hot-wire probes were placed centrally with respect to the side walls of the test section. All measurements were made above the test plate. The experimental study involved two aspects: verification that the expected laminar boundary layers were actually generated by comparison of boundary-layer velocity measurements with numerical predictions, and the testing of hot-element gages.

Boundary-Layer Study

Velocity measurements were made in the boundary layer by means of a hot-wire anemometer for both steady and oscillating flows. The velocity surveys conducted are described in Table 2. Calibration of the hot-wire probes was accomplished using a TSI Model 1125 airflow calibrator and standard calibration techniques. The data-acquisition system for velocity measurements is described in Fig. 6. The probe-positioning mechanism incorporated a dial micrometer to accurately position the hot wire relative to the plate surface. The wave generator wedge (Fig. 5) was locked at midstroke for steady-flow velocity surveys. The velocity at each y value in the survey was determined by programming the data-acquisition system to take 500 voltage readings, average the 500 readings, and evaluate the velocity from the hot-wire calibration curve. The wave generator was driven by an adjustable-speed electric motor for the oscillating flow studies. A flywheel on the wave generator drive shaft ensured a constant angular speed. The angular speed was monitored by an optical pickup focused on white markers on the flywheel. The uncertainty in oscillation frequency was $\pm0.5\%$.

Velocity measurements in oscillating flows were accomplished by use of a once-per-revolution trigger initiated at a fixed point in the cycle and sent to the voltmeter. The voltmeter was set to take readings at 20 equally spaced time intervals over the period of each cycle of oscillation on receiving the trigger signal. The voltage values were ensemble-averaged over a number of cycles and the 20 corresponding velocity values were determined from the hot-wire calibration curve. A cosine wave was also fit through the 20 velocity values to yield the velocity variation in the form of Eq. (2). Figure 7 displays typical ensemble-averaged velocity values and the corresponding cosine wave fits at two y values, one in and one outside the boundary layer, for an oscillating flow at a frequency of 10 Hz. The fitted curves closely match the data points in each case, and the velocity variation is clearly sinusoidal. Expressions for the fitted curves are given in the figure. Such expressions allowed accurate evaluation of the velocity and the phase-angle variation in the boundary layer.

Table 2 Experimental boundary-layer velocity surveys

Case	Test configuration	f, Hz	$\bar{\omega}$	$\phi_{\tau ex}$,[a] deg
A1	TC I	10.0	0.45	26
A2	TC II	3.00	0.25	11
A3	TC II	5.58	0.44	19
A4	TC II	10.0	0.78	31
A5	TC II	15.0	1.18	33
A6	TC II	20.0	1.59	35
B1	TC III	3.00	0.34	17
B2	TC III	10.0	1.19	30
B3	TC III	20.0	2.38	39
C1	TC I	Steady flow		
C2	TC II	Steady flow		

[a]Obtained by extrapolation of experimental ϕ_u profile.

Results for the oscillating-flow boundary-layer studies will be presented in terms of the ratio of mean velocities u_0/U_0, the oscillation amplitude ratio u_1/U_1, and the phase angle ϕ_u vs the similarity variable η. Due to the relative size of the test section and the thickness of the boundary layers on both the plate and the test-section side walls, a mild favorable pressure gradient was present in the flows generated in this study. This is evident by comparison of steady-flow boundary-layer velocity profiles with that for steady zero-pressure-gradient flows, the Blasius profile. Figures 8a and 8b show experimental results for oscillating flow cases A1 and A6, Table 2, in terms of u_0/U_0, u_1/U_1, and ϕ_u vs η, and the corresponding experimental steady-flow velocity profiles from cases C1 and C2, Table 2. The results in Fig. 8a were obtained using test configuation TC I, whereas those in Fig. 8b were obtained using test configuraion TC II. The mismatch between the steady-flow profile and the Blasius profile in each part of Fig. 8 indicates the presence of a pressure gradient. To model the pressure-gradient flows, the Falkner-Skan equation was used. This equation, which applies to the steady freestream flow, is

$$U(x) = Kx^{\beta/(2-\beta)} \tag{4}$$

where K is a constant and β is related to the strength of the pressure gradient. The value of β was found by comparing the experimental steady-velocity profiles with steady laminar boundary-layer profile solutions obtained numerically for various values of β. As shown in Fig. 8, the profile obtained for $\beta=0.20$ matches both steady experimental profiles. The same value of β applies to the other cases in Table 2.

Numerical solutions for oscillating-flow laminar boundary layers that correspond to the experimental cases studied were obtained using the method developed by Murphy and Prenter.[15] The method is a hybrid finite-element finite-difference scheme that is second-order accurate in x and t and fourth-order accurate in y. The mean pressure gradient for

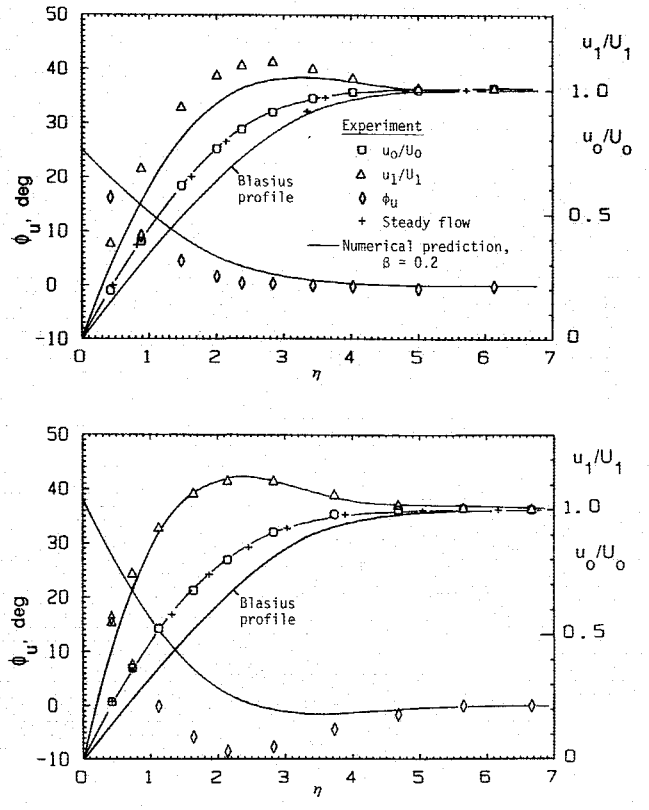

Fig. 8 Comparisons of measured and predicted velocity variations for steady and oscillating-flow laminar boundary layers: a) Case A1, $\bar{\omega}=0.45$, TC I; and b) Case A6; $\bar{\omega}=1.59$, TC II.

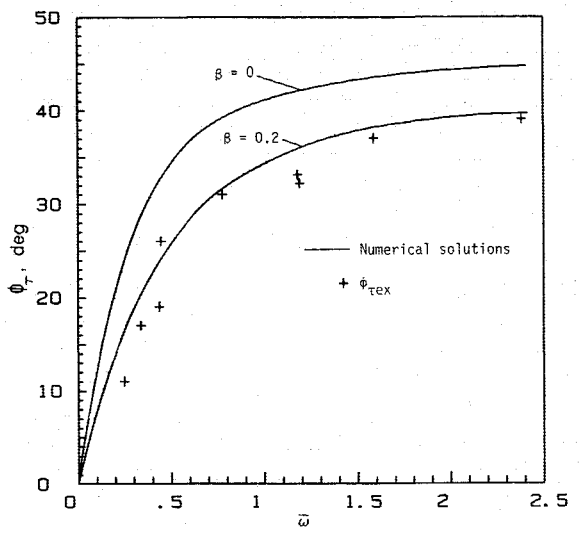

Fig. 9 Variations in ϕ_τ with $\bar{\omega}$.

oscillating flows was assumed to be that which existed in the corresponding steady flow. Figures 8a and 8b present representative comparisons of experimental and numerical results for the oscillating boundary-layer flows. These comparisons are for experimental cases obtained at two values of $\bar{\omega}$. In each part of the figure, the experimental results for u_0/U_0 vs η for the oscillating flow are in good agreement with the experimental steady-flow velocity profile, indicating no effect of flow oscillation on the mean velocity profile. This result has been observed in previous experimental studies of laminar oscillating flows.[16,17] The experimental and numerically predicted profiles for u_1/U_1 in Fig. 8a are in fair agreement, whereas in Fig. 8b the agreement between these profiles is good. Each profile exhibits values of u_1/U_1 that are larger than unity. The experimental and numerically predicted profiles for ϕ_u vs η in Fig. 8a are in fair agreement, whereas the profiles in Fig. 8b for ϕ_u differ somewhat. However, in each figure, extrapolation of the experimental ϕ_u profile to the wall to obtain ϕ_τ yields a value close to the corresponding numerically predicted value that is denoted as $\phi_{\tau n}$. Reference 18 presents graphs of experimental results similar to those in Fig. 8 for the remainder of the oscillating flow cases in Table 2. Extrapolation of the ϕ_u profile to obtain ϕ_τ for those cases also yields values close to the corresponding values of $\phi_{\tau n}$. Table 2 lists the value of ϕ_τ obtained by extrapolation of the experimental ϕ_u profile for each oscillating flow case. These values are denoted as $\phi_{\tau ex}$. Figure 9 presents a comparison of $\phi_{\tau ex}$ with $\phi_{\tau n}$ obtained for $\beta=0.2$. The scatter in $\phi_{\tau ex}$ is related to uncertainty in extrapolating the ϕ_u profiles. Although the values of $\phi_{\tau ex}$ tend to fall slightly below the curve, they support the validity of the numerical solution for ϕ_τ. Thus, it is concluded that ϕ_τ is reasonably well predicted by the numerical method. Also shown in Fig. 9 is the numerical solution for ϕ_τ vs $\bar{\omega}$ for zero-mean pressure-gradient flows ($\beta=0$) from Fig. 3. Comparison of this curve with the curve of ϕ_τ for $\beta=0.2$ shows that the variation of ϕ_τ with $\bar{\omega}$ is sensitive to the pressure gradient.

Measurement of ϕ_τ with Hot-Element Gages

Figure 10 describes the data-acquisition system used in conjunction with the hot-element gages to measure ϕ_τ. When subjected to an oscillating laminar flow, these gages produce a signal with a large dc component and a relatively small oscillating component. As a result, it was necessary to use a virtually noise-free dc power supply to operate the main anemometer unit and a high-quality ac-coupled transducer amplifier at the anemometer output to produce an adequate output signal. The ac coupling was acceptable since only the phase relation between the hot-wire signal and hot-element gage signal was of interest in the present investigation. The data acquisition system in Fig. 10 was used for processing signals from both the reference freestream hot wire and the wall hot-element gage in measuring ϕ_τ in order to eliminate a phase difference in output signals that might occur if separate signal processing systems were used. Two types of hot-element gages were tested in this study. One was the commercially available TSI model 1237 AU platinum film gage prepared by

Table 3 Hot-element gages tested

Designation	Type	Manufacturer	Element width W × Length L,[a] mm	Substrate
PF1	Platinum film	TSI, model 1237 AU	1.00×0.152	Quartz
PF2	Platinum film	TSI, model 1237 AU	1.00×0.152	Quartz
FW1	Flush-wire	NASA ARB[b]	1.75×0.01	Polysytrene
FW1	Flush-wire	NASA ARC	1.75×0.01	Polystyrene

[a]Length measured in flow direction; see Fig. 1. [b]Instrument Branch, NASA Ames Research Center.

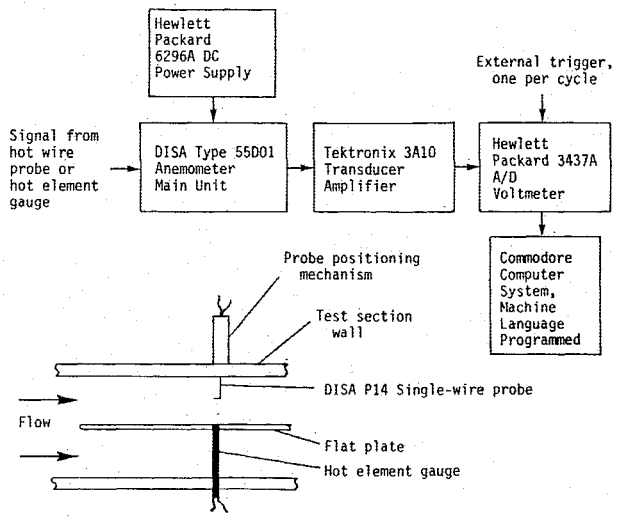

Fig. 10 Data-acquisition system for measurement of ϕ_τ.

depositing a thin platinum film on a quartz substrate. The other was a flush-wire gage prepared by the NASA Ames Research Center Instruments Branch by burying a 10 μm diameter wire flush with the surface of a polystyrene substrate. Flush-wire gages are described by Rubesin et al.[19] and Murthy and Rose.[20] Table 3 describes the hot-element gages tested. Four gages, two of each type, were tested. Table 4 describes the conditions under which experiments were conducted to measure ϕ_τ using the four hot-element gages. The platinum film gages were tested in flows with reduced frequencies ranging from 0.14 to 2.36. Failure of the hot elements of both flush-wire gages, apparently due to extended use, limited the testing of these gages to the cases noted in Table 4.

Measurements at fixed values of $\bar{\omega}$ revealed that ϕ_τ indicated by the gages depended on the overheat ratio (OHR), which ranged from 1.02 to 1.33. (OHR is defined here as the ratio of the hot-element operating resistance to the resistance of the element at the air temperature with no flow.) With few exceptions, the curves for ϕ_τ exhibited increasing values with increasing OHR until an approximately constant value was reached. The value of OHR beyond which ϕ_τ was constant tended to increase with increasing $\bar{\omega}$ and ranged from 1.05 to 1.20. The values of ϕ_τ obtained at OHR = 1.3 are denoted as $\phi_{\tau e}$ and are tabulated in Table 4.

A factor that affects the results for ϕ_τ indicated by the hot-element gages is the extent to which an exact match of the hot-element gage surface with the wall is obtained on installation of the gage. A small mismatch can have a significant effect on results. This matter was investigated for certain cases by repeating identical ϕ_τ measurement experiments, between which the hot-element gage in use was removed from the test configuration and reinstalled. At each installation, an optical magnifier was used to aid in matching the surfaces. This procedure was undertaken in four instances for platinum film gage PF2. These instances can be identified in Table 4 as cases PF2 B and C, PF2 E and F, PF2 I and J, and PF2 N and O. From Table 4, it is seen that the results for cases PF2 B and C differ by 1.2 deg, whereas those for cases PF2 E and F differ by about 3 deg. Results for cases PF2 I and J are the same, as are the results for cases PF2 N and O. Thus, results are reproducible within a few degrees when care is exercised in matching the surfaces.

Results obtained in this study also allow comparisons of results for similar gages tested under the same conditions. As noted in Table 4, results for cases PF1 A and PF2 E and F were obtained under the same test conditions. The same is true for cases PF1 B and PF2 N and O, cases FW1 A and FW2 B, and cases FW1 B and FW2 D. Differences in the results within each of these sets are small and are possibly caused by gage installation effects. Hence, within the uncertainty related to in-

Table 4 Hot-element gage ϕ_τ measurement cases.[a]

Case[b]	Test configuration	f, Hz	$\bar{\omega}$	$\phi_{\tau e}$[c]	$\phi_{\tau n} - \phi_{\tau e}$
PF1 A	TC I	10.0	0.45	15.3	8.8
PF1 B	TC II	20.0	1.66	25.8	12.8
PF2 A	TC I	3.00	0.14	−0.8	11.0
PF2 B	TC I	5.00	0.23	3.6	11.6
PF2 C	TC II	5.00	0.23	−4.8	10.6
PF2 D	TC I	7.00	0.32	10.8	8.4
PF2 E	TC I	10.00	0.45	13.3	10.8
PF2 F	TC I	10.00	0.45	16.2	7.9
PF2 G	TC I	20.00	0.90	18.2	15.2
PF2 H	TC II	3.00	0.25	4.4	12.0
PF2 I	TC II	5.45	0.45	12.4	11.2
PF2 J	TC II	5.45	0.45	12.4	11.2
PF2 K	TC II	7.00	0.58	15.3	12.2
PF2 L	TC II	10.00	0.83	18.9	13.3
PF2 M	TC II	10.90	0.90	22.0	11.2
PF2 N	TC II	20.00	1.66	24.9	13.8
PF2 O	TC II	20.00	1.66	24.9	13.8
PF2 P	TC III	3.00	0.35	7.0	13.2
PF2 Q	TC III	10.00	1.18	17.9	18.2
PF2 R	TC III	20.00	2.36	22.0	17.6
FW1 A	TC I	5.00	0.23	−5.5	20.4
FW1 B	TC I	10.00	0.45	9.5	14.2
FW1 C	TC I	20.00	0.90	17.3	15.8
FW2 A	TC II	3.00	0.14	−3.2	13.2
FW2 B	TC I	5.00	0.23	−2.5	17.7
FW2 C	TC I	7.0	0.32	4.3	14.9
FW2 D	TC I	10.00	0.45	10.4	13.0

[a]Angles are in degrees. [b]See Table 3 for gage designation code. [c]Obtained at OHR = 1.3.

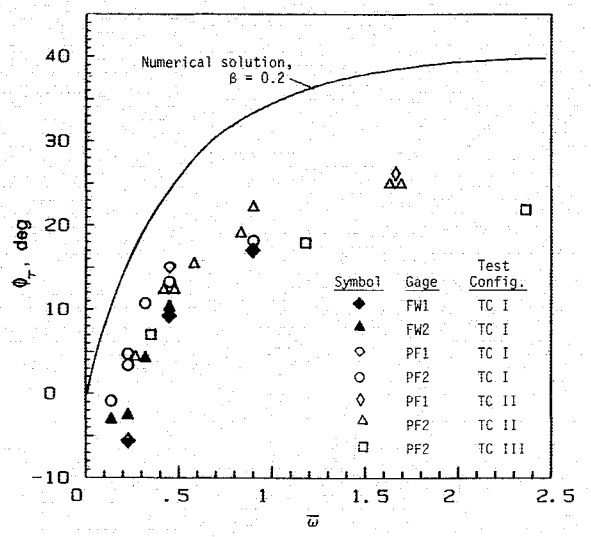

a) Comparison of numerical solution and experimental values for ϕ_τ

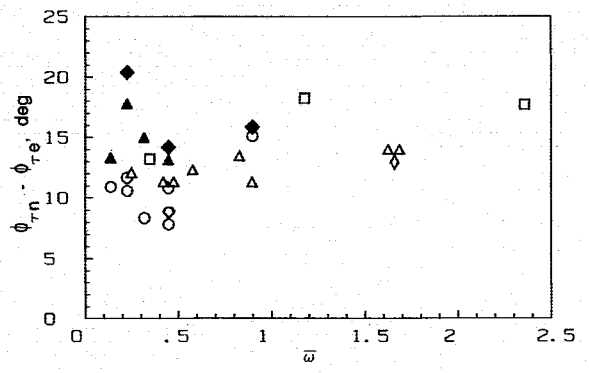

b) Difference between numerical solutions and experimental values for ϕ_τ

Fig. 11 Numerical and experimental results for wall shear stress phase angle.

stallation effects, no differences in results are apparent when different gages of the same type are used.

Comparison of Experimental and Numerically Predicted ϕ_τ

The next step is to compare experimental results for $\phi_{\tau e}$ indicated by the hot-element gages with the expected ϕ_τ variation. The latter is taken as the numerical prediction in Fig. 9 for $\beta = 0.2$. Figure 11a presents this comparison. It is evident from this figure that the experimental values of ϕ_τ are smaller than the corresponding predicted values. Thus, the wall shear-stress variation indicated by the hot-element gages lags the wall shear-stress variation for the boundary layer. In addition, the results indicate that the flush-wire gages tend to yield smaller values for ϕ_τ than do the platinum film gages when the gages are operated under the same conditions.

The results in Fig. 11a can be further examined by plotting the differences between the expected variation in ϕ_τ, $\phi_{\tau n}$, and experimental values of ϕ_τ. These differences are presented in Table 4 and plotted vs $\bar{\omega}$ in Fig. 11b for the four gages tested. Results in this form again display the differences between ϕ_τ values measured by flush-wire gages and those measured by platinum film gages. For the range of $\bar{\omega}$ covered for the flush-wire gages, the flush-wire data show that the shear-stress variation as indicated by these gages lags the expected shear-stress variation by about 17 deg, with an uncertainty of about ±4 deg. The data are too limited to indicate a trend with $\bar{\omega}$. Results for the platinum film gages show that the wall shear-stress variation indicated by these gages lags the expected shear-stress variation by an angle that tends to increase with $\bar{\omega}$. The uncertainty for the platinum film gage results relative to the central trend of the data is about ±4 deg.

The literature cited here provides insight into the causes of the phase lag in the gage response that is evident in Fig. 11. As noted, the study of Cole and Beck indicates that for airflow over a hot-element gage with a quartz substrate, unsteady heat transfer in the substrate is the predominant factor in the gage response. The investigation by Mao and Hanratty provides a means to verify this. They present an analysis that deals with the effect of unsteadiness in the fluid on the phase angle indicated by both heat-transfer- and mass-transfer-type gages. A phase angle correction θ to account for the fluid-related lag in the gage response relative to the true wall shear-stress variation is obtained in terms of a single dimensionless variable. When written for hot-element gages operating in laminar oscillating flows, their result (Fig. 3 of Ref. 9) takes the form

$$\theta = f(z)$$

where

$$z = (\omega/S)\,(SL_{\text{eff}}^2/\alpha_f)^{1/3}$$

In this expression, $S = (\partial u/\partial y)$ at the wall, α_f is the fluid thermal diffusivity, and L_{eff} is the length of the heated region in the direction of flow, which is estimated to be several times the hot-element length L. Since platinum film gages had the largest L value, they were selected for estimating the corrections for the present results. The corrections were determined by assuming $L_{\text{eff}} = 5L$. Flows produced in test configuration TC III yielded the largest values of θ. At the highest frequency of oscillation, 20 Hz, the correction was 1 deg. At lower values of frequency, the correction was smaller than 1 deg. Thus, although there is some uncertainty in the value of the phase-angle correction obtained from this analysis, the corrections are small compared to the differences $\phi_{\tau n} - \phi_{\tau e}$ in Fig. 11b. It is concluded that, for the conditions of this investigation, the observed lag in the output signal for both the platinum film and flush-wire gages is primarily due to unsteady heat-conduction effects in the substrate.

Concluding Remarks

The results of this study indicate that when hot-element gages of the type tested are used to measure wall shear stress in periodic flows, there is an inherent time lag of the gage signal relative to the true wall shear-stress variation. If the correct phase relation for time-dependent wall shear stress is to be obtained from gage output, a frequency-response correction is required. Unsteady heat conduction in the gage substrate plays a significant role in producing the lag in gage response. For the laminar oscillating flows studied here, substrate heat conduction dominates. For laminar oscillating flows similar to those generated in this study, the results in Fig. 11b provide, for each type of gage, frequency-response corrections for the wall shear-stress phase angle ϕ_τ. These results, however, may not be applicable to other periodic flows.

Acknowledgment

This study was supported by the NASA Ames Research Center, Moffett Field, CA, under Grant No. NCC 2-200.

References

[1]Goldstein, R. J., *Fluid Mechanics Measurements*, Hemisphere, New York, 1983.

[2]Acharya, M., Bornstein, M. P., and Vokurka, V., "Development of a Floating Element for Measurement of Surface Shear Stress," *AIAA Journal*, Vol. 23, March 1984, pp. 410–415.

[3]Bellhouse, B. J. and Schultz, D. L., "Determination of Mean and Dynamic Skin Friction, Separation, and Transition in Low-Speed

Flow with a Thin-Film Heated Element," *Journal of Fluid Mechanics,* Vol. 24, Feb. 1966, pp. 379–400.

[4]Kobashi, Y., and Hayakawa, M., "Structure of Turbulent Boundary Layer on an Oscillating Flat Plate," *Unsteady Turbulent Shear Flows,* edited by R. Michel, J. Cousteix, and R. Houdeville, Springer-Verlag, New York, 1981.

[5]Ramaprian, B. R. and Tu, S. W., "Study of Periodic Turbulent Pipe Flows," Iowa Inst. of Hydraulic Res., Iowa City, IA, Rept. 238, 1982.

[6]Simpson, R. L., Shivaprasad, B. G., and Chew, Y. T., "The Structure of a Separating Turbulent Boundary Layer, Part 4: Effects of Periodic Free-Stream Unsteadiness," *Journal of Fluid Mechanics,* Vol. 127, Feb. 1983, pp. 219–261.

[7]Dewey, C. F., Jr. and Huber, P. W., "Measurement Methods for Fluid Shear Stress," Fluid Mechanics Lab. Publications, MIT, Cambridge MA, 1982.

[8]Hanratty, T. J. and Campbell, J. A., "Measurement of Wall Shear Stress," *Fluid Mechanics Measurements,* Hemisphere, New York, 1983.

[9]Mao, Z.-X. and Hanratty, T. J., "The Use of Scalar Transport Probes to Measure Wall Shear Stress in a Flow with Imposed Oscillations," *Experiments in Fluids,* Vol. 3, 1985, pp. 129–135.

[10]Menendez, A. N. and Ramaprian, B. R., "The Use of Flush-Mounted Hot-Film Gauges to Measure Skin Friction in Unsteady Boundary Layers," *Journal of Fluid Mechanics,* Vol. 161, Dec. 1985, pp. 139–159.

[11]Cole, K. D. and Beck, J. V., "Conjugated Heat Transfer from a Strip Heater with the Unsteady Surface Element Method," AIAA Paper 86-1242, June 1986.

[12]Cousteix, J., Houdeville, R., and Javelle, J., "Response of a Turbulent Boundary Layer to a Pulsation of the External Flow With and Without Adverse Pressure Gradient," *Unsteady Turbulent Shear Flows,* edited by R. Michel, J. Cousteix, and R. Houdeville, Springer-Verlag, New York, 1981.

[13]Lighthill, M. J., "The Response of Laminar Skin Friction and Heat Transfer to Fluctuations in the Stream Velocity," *Proceedings of the Royal Society,* Series A, Vol. 224, June 1954, pp. 1–23.

[14]Cebeci, T. and Carr, L. W., "A Computer Program for Calculating Laminar and Turbulent Boundary Layers for Two-Dimensional Time Dependent Flows," NASA TM-78470, March 1978.

[15]Murphy, J. D. and Prenter, P. M., "A Hybrid Computing Scheme for Unsteady Turbulent Boundary Layers," *3rd Symposium on Turbulent Shear Flows,* Univ. of California, Davis, Sept. 1981.

[16]Hill, P. G. and Stenning, A. H., "Laminar Boundary Layers in Oscillating Flows," *Journal of Basic Engineering,* Vol. 82, Sept. 1960, pp. 593–608.

[17]Karlsson, S. K. F., "An Unsteady Turbulent Boundary Layer," *Journal of Fluid Mechanics,* Vol. 5, 1959, pp. 622–636.

[18]Giddings, T. A. and Cook, W. J., "Response of Hot Element Flush Wall Gages in Oscillating Laminar Flow," Iowa State Engr. Res. Inst., Rept. ISU-ERI-Ames-86435, Feb. 15, 1986.

[19]Rubesin, M. W., Okuno, A. F., Mateer, G. G., and Brosh, A., "A Hot-Wire Surface Gage for Skin Friction and Separation Detection Measurements," NASA TM X-62, 1975.

[20]Murthy, V. S. and Rose, W. C., "Buried Wire Gage for Wall Shear Stress Measurements," AIAA 10th Aerodynamic Testing Conf., San Diego, CA, April 19–21, 1978.